Overcoming Kinetic Barriers of Remote Electrochemiluminescence on Boron-Doped Diamond via Catalytic Coreactant Oxidation

Alessandro Fracassa,[a] Chiara Mariani,[a] Andrea Fiorani,[b] Yasuaki Einaga,[b] Conor F. Hogan,[c] Francesco Paolucci,[a,d] Neso Sojic,[e] Paul S. Francis,*[f] and Giovanni Valenti*[a]

a. Department of Chemistry "Giacomo Ciamician", Alma Mater Studiorum – University of Bologna, Via Gobetti 85, 40129 Bologna, Italy.

b. Department of Chemistry, Keio University, 3-14-1 Hiyoshi, Yokohama 223-8522, Japan.

c. The Biomedical and Environmental Sensor Technology (BEST) Research Centre, Biosensors Program, La Trobe Institute for Molecular Science (LIMS), La Trobe University, Melbourne, 3086, VIC, Australia.

d. ICMATE-CNR, Corso Stati Uniti 4, 35127 Padova, Italy.

e. Univ. Bordeaux, CNRS, Bordeaux INP, ISM, UMR 5255, ENSCBP, 33607, Pessac, France.

f. Centre for Sustainable Bioproducts, Faculty of Science, Engineering and Built Environment, Deakin University, Geelong, Victoria 3220, Australia.

Electronic Supporting Materials

Table of Contents

Experimental Information

Chemicals

Bis(2,2′-bipyridine)-4′-methyl-4-carboxybipyridine-ruthenium *N*-succinimidyl ester-bis(hexafluorophosphate) (MW = 1014.66 g mol^{-1}, BioReagent), tri-*n*-propylamine (TPrA, MW = 143.27 g mol^{-1}, ≥98%), lithium perchlorate ($LiClO_4$, MW = 106.39 g mol^{-1}, ≥98%), sodium phosphate monobasic dihydrate ($NaH_2PO_4 \cdot 2H_2O$, MW = 156.01 g mol^{-1}, ≥99%), sodium phosphate dibasic (Na_2HPO_4, MW = 141.96 g mol^{-1}, ≥99.5%), and phosphoric acid (H_3PO_4, MW = 98.00 g mol^{-1}, ≥85%) were purchased from Sigma-Aldrich. $Na_3[Ir(sppy)_3]$ was purchased from Luminescence Technology Corp. Amine functionalized 2.8 µm polystyrene beads (Dynabeads™ M-270 Amine) were purchased from Thermo Fisher Scientific Inc.

Preparation of the BDD Electrode

BDD films were deposited on silicon (111) wafers (Shinwa Tsusho, Japan) using a microwave plasma-assisted chemical vapor deposition (MPCVD) system (CORNES Technologies/ASTeX-5400). Acetone and trimethyl borate were used as the carbon and boron sources, respectively, with a B/C atomic ratio of 1%. Details on BDD electrode characterization are available in literature.[1]

Working Electrode Cleaning and Pretreatment

Prior to each measurement, the BDD surface was electrochemically cleaned through three cyclic voltammetry scans in 0.1 M $LiClO_4$. The potential was swept at 200 $mV \cdot s^{-1}$ between +3.5 V and -3.5 V, starting from the open circuit potential. After cleaning, the BDD electrode was pretreated to regulate the surface termination and ensure reproducibility: (i) cathodic reduction at −3.5 V followed by anodic oxidation at +3.5 V (AO-BDD) or (ii) anodic oxidation at +3.5 V followed by cathodic reduction at −3.5 V (CR-BDD), in 0.1 M $LiClO_4$ solution. Details on the characterization of both surface terminations are available in literature.[2,3]

Beads preparation

5 µL of beads stock suspension (30 $mg \cdot mL^{-1}$) were washed three times with 200 µL of 0.3 M phosphate buffer (PB, pH 6.8) with <0.1% surfactant. Subsequently, 150 µL of a 1 mM solution of Ru(II) complex (5 Ru(II) complex equivalents per NH_2) in 0.3 M PB (pH 6.8) with <0.1% surfactant were added to the beads suspension. The mixture was incubated overnight at room temperature under physical mixing at 1100 rpm by ZX3 Advanced Vortex Mixer (VELP Scientifica Srl, Italy). After incubation, the beads were washed with 200 µL of 0.3 M PB (pH 6.8) with <0.1% surfactant for 5 times. Finally, Ru(II)-labeled beads were suspended in 208 µL of 0.3 M PB (pH 6.8) with <0.1% surfactant to a final concentration of 0.72 $mg \cdot mL^{-1}$ and stored at 4°C.

Electrochemiluminescence

In the microscopy setup, the ECL and optical images were captured following the deposition of a suspension of Ru(II) covalently functionalized beads in the electrochemical cell where the microspheres were collected on the working electrode surface using a magnet placed underneath. The ECL and optical imaging was performed using solutions of 180 mM TPrA in 0.3 M PB (pH 6.8), with or without the addition of 100 µM $[Ir(sppy)_3]^{3-}$, in a PTFE homemade electrochemical cell comprising a BDD working (3.5 cm^2), Pt counter, and Ag/AgCl (3 M KCl) reference electrodes. The different solutions were inserted in the electrochemical cell with a pressure-driven flow controller (OB1 Mk3, Elveflow) equipped with a flux sensor (Flow-04D working range from 0 to 1000 µL min^{-1}) and exchanged, when necessary, with a 10-way bidirectional valve (MUX distributor). For microscopic imaging, an epifluorescence microscope from Nikon (Chiyoda, Tokyo, Japan) equipped with an ultrasensitive EMCCD camera (EM-CCD 9100−13 from Hamamatsu, Japan) was used with a resolution of 512 × 512 pixel and a size of 16 × 16 μm^2. The microscope was enclosed in a homemade dark box to avoid

interferences from external light. It was also equipped with a motorized microscope stage (Corvus, Märzhauser, Wetzlar, Germany) for sample positioning and with water-dipping objective from Nikon (magnification 100×/NA 1.10/WD (mm) 2.5). Additionally, the integrated system included a SP-300 potentiostat (BioLogic Science Instrument, France) triggered with the camera. CV-ECL plots were collected by scanning the working electrode potential at 100 $mV \cdot s^{-1}$ from open circuit potential (OCP) up to 4 V (*vs* Ag/AgCl 3 M KCl), back to 0 V (*vs* Ag/AgCl 3 M KCl) and, eventually, terminating the cycle at OCP. The beads emission during CV-ECL measurements was acquired every 200 ms to follow the temporal evolution of the signal. The integration time of the EM-CCD camera was set to 200 ms. ECL images were captured by applying a double chronoamperometric pulse: OCP for 2 s and 1.1 V or 2.2 V (*vs* Ag/AgCl 3M KCl) for the next 5 s. The total integration time of the EM-CCD camera was set to 7 s. Unless otherwise stated, gain and sensitivity parameters of the EM-CCD camera were set to 1 and 255, respectively.

Reaction schemes

$$TPrA \rightleftharpoons TPrA^{\bullet +} + e^{-} \quad \text{(S1)}$$

$$[Ir(sppy)_3]^{3-} \rightleftharpoons [Ir(sppy)_3]^{2-} + e^{-} \quad \text{(S2)}$$

$$[Ir(sppy)_3]^{2-} + TPrA \rightarrow [Ir(sppy)_3]^{3-} + TPrA^{\bullet +} \quad \text{(S3)}$$

$$TPrA^{\bullet +} \rightarrow TPrA^{\bullet} + H^{+} \quad \text{(S4)}$$

$$[Ir(sppy)_3]^{2-} + TPrA^{\bullet} \rightarrow [Ir(sppy)_3]^{3-*} + Im^{+} \quad \text{(S5)}$$

$$[Ir(sppy)_3]^{3-*} \rightarrow [Ir(sppy)_3]^{3-} + hv\ (515\ nm) \quad \text{(S6)}$$

$$[Ru(bpy)_3]^{2+} + TPrA^{\bullet} \rightarrow [Ru(bpy)_3]^{+} + Im^{+} \quad \text{(S7)}$$

$$[Ru(bpy)_3]^{+} + [Ir(sppy)_3]^{2-} \rightarrow [Ru(bpy)_3]^{2+*} + [Ir(sppy)_3]^{3-} \quad \text{(S8)}$$

$$[Ru(bpy)_3]^{+} + TPrA^{\bullet +} \rightarrow [Ru(bpy)_3]^{2+*} + TPrA \quad \text{(S9)}$$

$$[Ru(bpy)_3]^{2+*} \rightarrow [Ru(bpy)_3]^{2+} + hv\ (620\ nm) \quad \text{(S10)}$$

Scheme S1. Photophysically and energetically feasible reactions between $[Ru(bpy)_3]^{2+}$, $[Ir(sppy)_3]^{3-}$ and TPrA reaction partners.

ECL images elaboration

ECL data points represented in CV-ECL were determine from ECL images captured every 200 ms during the potential scan. For each frame, 14.28 × 0.63 µm regions of interest (ROI) centered on the beads were isolated (see Fig. 3 and Fig. S5). ECL profiles of single emitting beads within the selected ROI were plotted and peak values were averaged (n. beads ≥ 4). The background signal is removed by subtracting to the averaged ECL intensity, for each frame, the ECL profile peak value retrieved over a 14.28 × 0.63 µm ROI centered in a region where no beads are present. The resulting values were eventually plotted as function of the applied potential. ECL values collected during double-step CA for statistical analysis were retrieved similarly. The same ROI were used to extract raw ECL intensity profiles along the radial direction. To remove the background signal, the ECL intensity points within the first 1.59 µm from the ECL profiles edge, where no bead emission was detected, were averaged and the so-obtained average was subtracted to the raw profiles to isolate the ECL signal from $[Ru(bpy)_3]^{2+}$ labels. The peak values of the so-elaborated ECL profile from each bead were further used for statistical analysis in Fig. 3 and Fig. S5.

CV-ECL of Ru@Beads and Ru@Beads/$[Ir(sppy)_3]^{3-}$ on CR-BDD

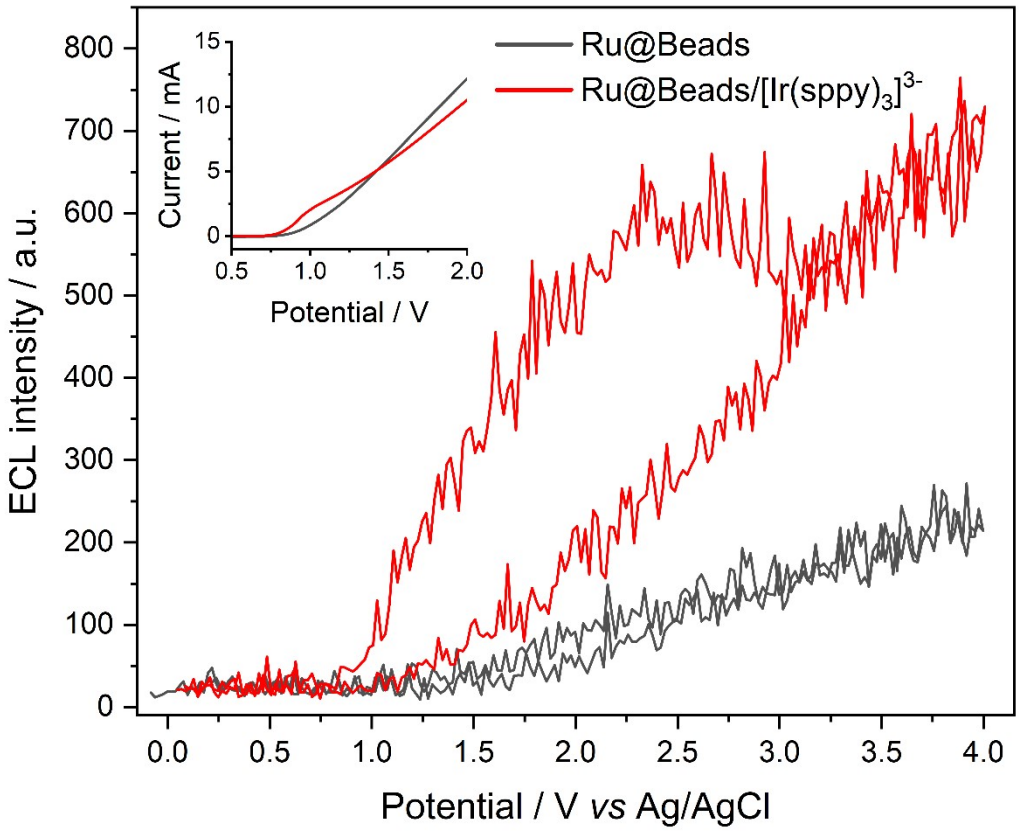

Figure S1. CV-ECL of Ru@Beads (grey line) and Ru@Beads/$[Ir(sppy)_3]^{3-}$ (red line) on CR-BDD. The potential was scanned at 100 $mV \cdot s^{-1}$ from open circuit potential (OCP) up to 4 V, back to 0 V, and eventually terminating the cycle at OCP. ECL data points were determined as reported in the paragraph "ECL images elaboration" by elaborating ECL images captured every 200 ms during potential scan. Inset: LSV *i-V* curves for Ru@Beads (grey line) and Ru@Beads/$[Ir(sppy)_3]^{3-}$ (red line) on CR-BDD.

Cyclic voltammetry of Ru@Beads on AO-BDD and CR-BDD

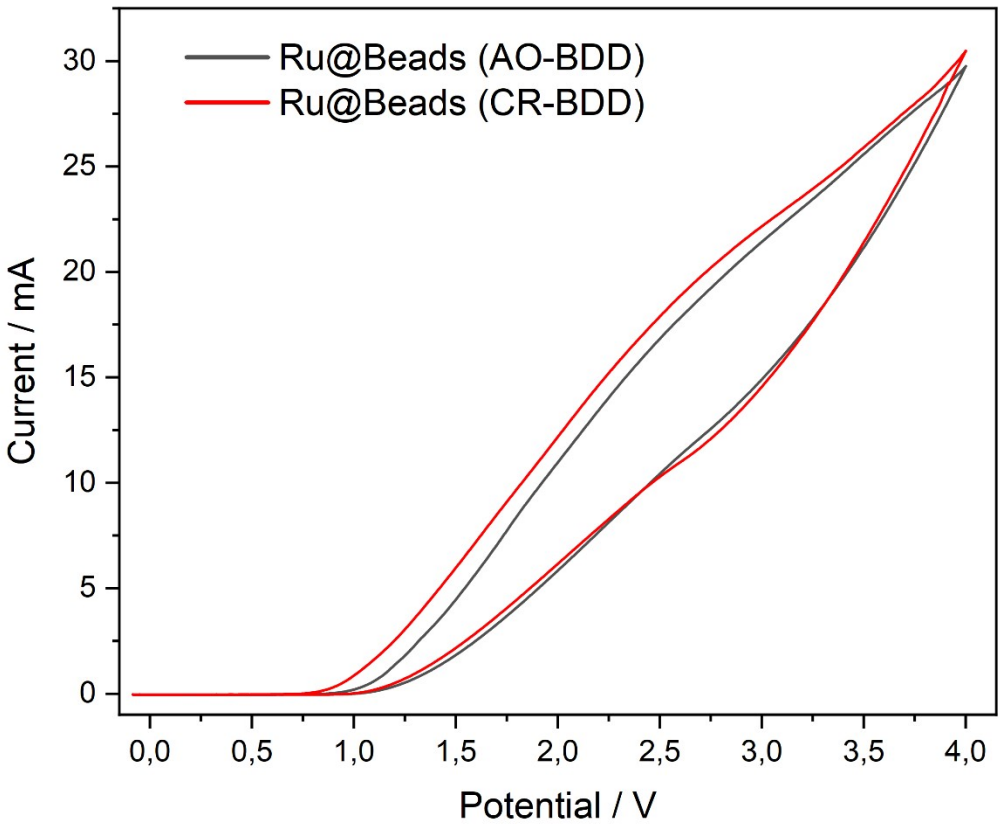

Figure S2. Cyclic voltammograms of Ru@Beads on AO-BDD (grey line) and CR-BDD (red line) electrodes. Scan rate: 100 $mV \cdot s^{-1}$.

Cyclic voltammetry of Ru@Beads and Ru@Beads/$[Ir(sppy)_3]^{3-}$ on AO-BDD

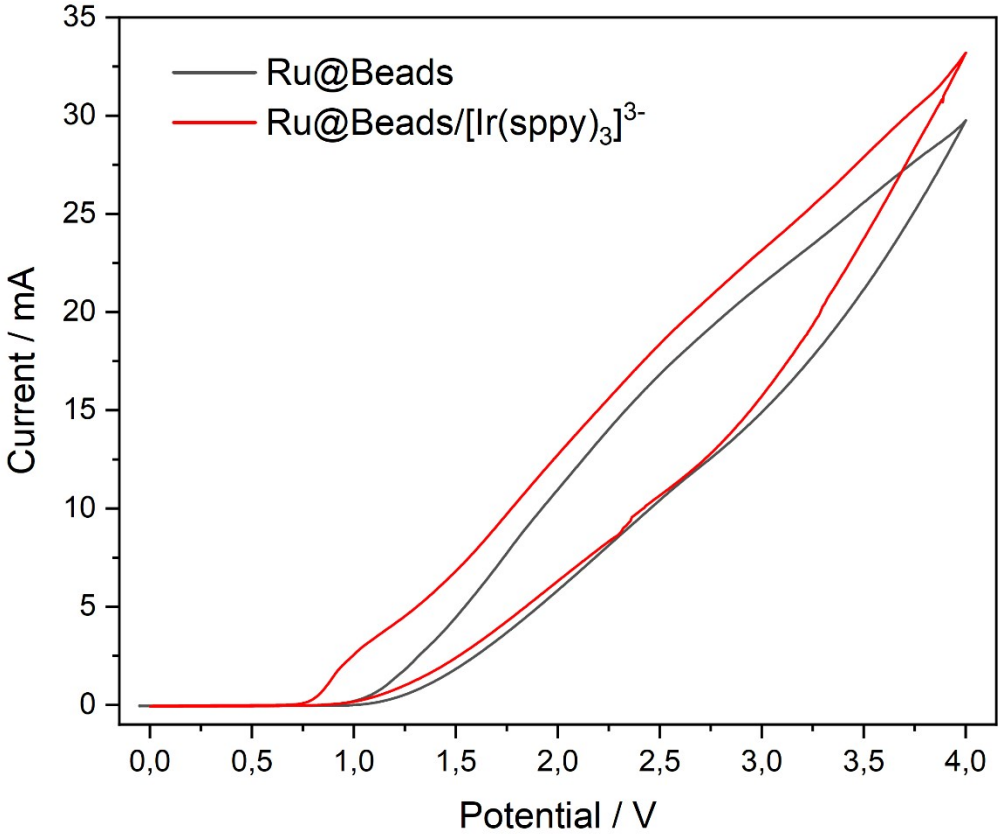

Figure S3. Cyclic voltammograms of Ru@Beads (grey line) and Ru@Beads/$[Ir(sppy)_3]^{3-}$ (red line) on AO-BDD electrode. Scan rate: 100 $mV \cdot s^{-1}$.

Bright field image of Ru@Bead at 1.1 V

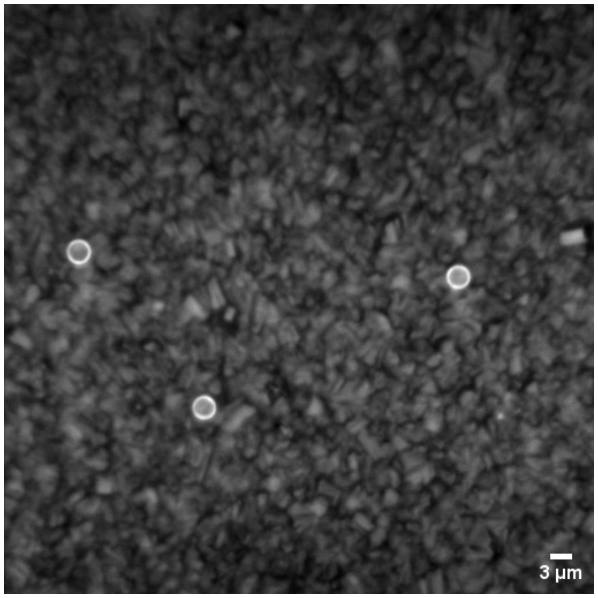

Figure S4. Bright field image of 2.8 µm beads covalently labelled with $[Ru(bpy)_3]^{2+}$ in a 0.3 M PB solution (pH 6.8) with 180 mM TPrA. This image is the bright field counterpart of the ECL image in Fig. 3a. The image was captured with a CCD camera for a total integration time of 200 ms. Magnification, 100×; objective numerical aperture, 1.1; scale bar, 3 µm.

ECL images and statistical analysis of Ru@Bead and Ru@Bead/$[Ir(sppy)_3]^{3-}$ at 2.2 V

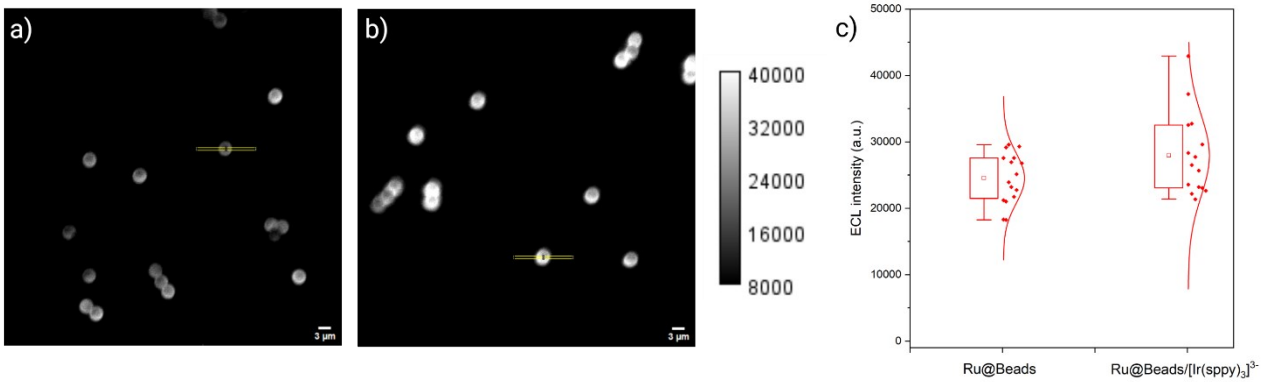

Fig. S5. ECL images of 2.8 µm beads covalently labelled with $[Ru(bpy)_3]^{2+}$ in a 0.3 M PB solution (pH 6.8) with 180 mM TPrA (a) without (Ru@Beads) and (b) with 100 µM $[Ir(sppy)_3]^{3-}$ (Ru@Beads/$[Ir(sppy)_3]^{3-}$) on AO-BDD. The images were captured with an EM-CCD camera by recording the ECL signal for 7 s during a two-step chronoamperometry measurement: 2 s at open circuit potential (OCP) and 5 s at 2.2 V *vs* Ag/AgCl. Magnification, 100×; objective numerical aperture, 1.1; gain, 1; sensitivity, 255; contrast scale, 8000 to 40000; scale bar, 3 µm. The yellow rectangles (14.28 x 0.63 µm) centered on the beads represent the ROI used to compute the ECL profiles of single beads (see "ECL images elaboration"). c) Statistical analysis of ECL profiles peak values obtained from Ru@Beads (left, n = 16) and Ru@Beads/$[Ir(sppy)_3]^{3-}$ (right, n = 15).

References

1 K. Sakanoue, A. Fiorani, C. I. Santo, Irkham, G. Valenti, F. Paolucci and Y. Einaga, *ACS Sensors*, 2022, **7**, 1145–1155.

2 S. Kasahara, K. Natsui, T. Watanabe, Y. Yokota, Y. Kim, S. Iizuka, Y. Tateyama and Y. Einaga, *Anal. Chem.*, 2017, **89**, 11341–11347.

3 S. Kasahara, T. Ogose, N. Ikemiya, T. Yamamoto, K. Natsui, Y. Yokota, R. A. Wong, S. Iizuka, N. Hoshi, Y. Tateyama, Y. Kim, M. Nakamura and Y. Einaga, *Anal. Chem.*, 2019, **91**, 4980–4986.